DOI: 10.1021/ic901169p

Inorganic Chemistry
Article

Four New Lanthanide−Nitronyl Nitroxide (Ln^{III} = Pr^{III}, Sm^{III}, Eu^{III}, Tm^{III}) Complexes and a Tb^{III} Complex Exhibiting Single-Molecule Magnet Behavior

Jin-Xia Xu,[†] Yue Ma,[†] Dai-zheng Liao,*[,†] Gong-Feng Xu,[‡] Jinkui Tang,*[,‡] Chao Wang,[†] Na Zhou,[†] Shi-Ping Yan,[†] Peng Cheng,[†] and Li-Cun Li[†]

[†]*Department of Chemistry, Nankai University, Tianjin 300071, P. R. China, and* [‡]*State Key Laboratory of Rare Earth Resource Utilization, Changchun Institute of Applied Chemistry, Chinese Academy of Sciences, Changchun 130022, P. R. China*

Received June 17, 2009

Five new complexes based on rare-earth-radical $[Ln(hfac)_3(NIT\text{-}5\text{-}Br\text{-}3py)]_2$ (Ln=Pr (**1**), Sm (**2**), Eu (**3**), Tb (**4**), Tm (**5**); hfac = hexafluoroacetylacetonate; NIT-5-Br-3py = 2-(4,4,5,5-tetramethyl-3-oxylimidazoline-1-oxide)-5-bromo-3-pyridine) have been synthesized and characterized by X-ray crystal diffraction. The single-crystal structures show that these complexes have similar structures, in which a NIT-5-Br-3py molecule acts as a bridging ligand linking two Ln(III) ions through the oxygen atom of the N−O group and nitrogen atom from the pyridine ring to form a four-spin system. Both static and dynamic magnetic properties were measured for complex **4**, which exhibits single-molecule magnetism behavior.

Introduction

Lanthanide complexes have sparked increasing interesting in past decades because of their special properties: porous, magnetic, optical, and electronic.[1] In the field of molecule-based magnetic materials, on one hand, a number of mixed transition-metal/ lanthanide complexes (3d−4f) have been obtained.[2] On the other hand, the lanthanide compounds involving organic radicals (2p−4f) have attracted much attention in recent years.[3] The stable nitronyl nitroxides radicals (NITR) are widely used because they can act as not only spin carriers but also building blocks. Several

*To whom correspondence should be addressed. E-mail: liaodz@nankai.edu.cn (D.-Z.L.); tang@ciac.jl.cn (J.-K.T.).

(1) (a) Reineke, T. M.; Eddaoudi, M.; Fehr, M.; Kelley, D.; Yaghi, O. M. *J. Am. Chem. Soc.* **1999**, *121*, 1651. (b) Reineke, T. M.; Eddaoudi, M.; O'Keefe, M.; Yaghi, O. M. *Angew. Chem., Int. Ed.* **1999**, *38*, 2590. (c) Pan, L.; Huang, X. Y.; Li, J.; Wu, Y. G.; Zheng, N. W. *Angew. Chem., Int. Ed.* **2000**, *39*, 527. (d) Pan, L.; Adams, K. M.; Hernandez, H. E.; Wang, X. T.; Zheng, C.; Hattori, Y.; Kaneko, K. *J. Am. Chem. Soc.* **2003**, *125*, 3062. (e) Ma, B. Q.; Zhang, D. S.; Gao, S.; Jin, T. Z.; Yan, C. H.; Xu, G. X. *Angew. Chem., Int. Ed.* **2000**, *39*, 3644. (f) Long, D. L.; Blake, A. J.; Champness, N. R.; Wilson, C.; Schröder, M. *Angew. Chem., Int. Ed.* **2001**, *40*, 2444. (g) Goodgame, D. M. L.; Grachvogel, D. A.; White, A. J. P.; Williams, D. J. *Inorg. Chem.* **2001**, *40*, 6180. (h) Dalgarno, S. J.; Raston, C. L. *Chem. Commun.* **2002**, 2216. (i) Gheorghe, R.; Andruh, M.; Müller, A.; Schmidtmann, M. *Inorg. Chem.* **2002**, *41*, 5314. (j) Vaidhyanathan, R.; Natarajan, S.; Rao, C. N. R. *Inorg. Chem.* **2002**, *41*, 4496. (k) Almeida Paz, F. A.; Klinowski, J. *Chem. Commun.* **2003**, 1484. (l) Ghosh, S. K.; Bharadwaj, P. K. *Inorg. Chem.* **2005**, *44*, 3156. (m) Gándara, F.; García-Cortés, A.; Cascales, C.; Gómez-Lor, B.; Gutiérrez-Puebla, E.; Iglesias, M.; Monge, A.; Snejko, N. *Inorg. Chem.* **2007**, *46*, 3475. (n) Robin, A. Y.; Fromm, K. M. *Coord. Chem. Rev.* **2006**, *250*, 2127.

(2) (a) Prasad, T. K.; Rajasekharan, M. V.; Costes, J. P. *Angew. Chem., Int. Ed.* **2007**, *46*, 2851. (b) Wang, F. Q.; Zheng, X. J.; Wan, Y. H.; Sun, C. Y.; Wang, Z. M.; Wang, K. Z.; Jin, L. P. *Inorg. Chem.* **2007**, *46*, 2956. (c) Pointillart, F.; Bernot, K.; Sessoli, R.; Gatteschi, D. *Chem.—Eur. J.* **2007**, *13*, 1602. (d) Liu, F. C.; Zeng, Y. F.; Jiao, J.; Li, J. R.; Bu, X. H.; Ribas, J.; Batten, S. R. *Inorg. Chem.* **2006**, *45*, 6129. (e) Figuerola, A.; Ribas, J.; Solans, X.; Font-Bardia, M.; Maestro, M.; Diaz, C. *Eur. J. Inorg. Chem.* **2006**, *9*, 1846. (f) Shi, W.; Chen, X. Y.; Zhao, B.; Yu, A.; Song, H. B.; Cheng, P.; Wang, H. G.; Liao, D. Z.; Yan, S. P.; Jiang, Z. H. *Inorg. Chem.* **2006**, *45*, 3949. (g) Shi, W.; Chen, X. Y.; Zhao, Y. N.; Zhao, B.; Cheng, P.; Yu, A.; Song, H. B.; Wang, H. G.; Liao, D. Z.; Yan, S. P.; Jiang, Z. H. *Chem.—Eur. J.* **2005**, *11*, 5031. (h) Yue, Q.; Yang, J.; Li, G. H.; Li, G. D.; Xu, W.; Chen, J. S.; Wang, S. N. *Inorg. Chem.* **2005**, *44*, 5241. (i) Zhao, B.; Cheng, P.; Chen, X. Y.; Cheng, C.; Shi, W.; Liao, D. Z.; Yan, S. P.; Jiang, Z. H. *J. Am. Chem. Soc.* **2004**, *126*, 3012. (j) Benelli, C.; Gatteschi, D. *Chem. Rev* **2002**, *102*, 2369.

(3) (a) Kaizaki, S.; Shirotani, D.; Tsukahara, Y.; Nakata, H. *Eur. J. Inorg. Chem.* **2005**, 3503. (b) Tsukuda, T.; Suzuki, T.; Kaizaki, S. *J. Chem. Soc., Dalton Trans.* **2002**, 1721. (c) Lescop, C.; Luneau, D.; Rey, P.; Bussière, G.; Reber, C. *Inorg. Chem.* **2002**, *41*, 5566. (d) Poneti, G.; Bernot, K.; Bogani, L.; Caneschi, A.; Sessoli, R.; Wernsdorferc, W.; Gatteschia, D. *Chem. Commun.* **2007**, 1807. (e) Bernot, K.; Bogani, L.; Caneschi, A.; Gatteschi, D.; Sessoli, R. *J. Am. Chem. Soc.* **2006**, *128*, 7947. (f) Bogani, L.; Sangregorio, C.; Sessoli, R.; Gatteschi, D. *Angew. Chem., Int. Ed.* **2005**, *44*, 5817. (g) Bernot, K; Luzon, J.; Bogani, L.; Etienne, M.; Sangregorio, C.; Shanmugam, M.; Caneschi, A.; Sessoli, R.; Gatteschi, D. *J. Am. Chem. Soc.* **2009**, *131*, 5573.

(4) (a) Osa, S.; Kido, T.; Matsumoto, N.; Re, N.; Pochaba, A.; Mrozinski, J. *J. Am. Chem. Soc.* **2004**, *126*, 420. (b) Mori, F.; Nyui, T.; Ishida, T.; Nogami, T.; Choi, K.-Y.; Nojiri, H. *J. Am. Chem. Soc.* **2006**, *128*, 1440. (c) Aronica, C.; Pilet, G.; Chastanet, G.; Wernsdorfer, W.; Jacquot, J.-F.; Luneau, D. *Angew. Chem.* **2006**, *118*, 4775. (d) Costes, J.-P.; Shova, S.; Wernsdorfer, W. *Dalton Trans.* **2008**, 1843. (e) Ishikawa, N.; Sugita, M.; Ishikawa, T.; Koshihara, S.; Kaizu, Y. *J. Am. Chem. Soc.* **2003**, *125*, 8694. (f) Tang, J.; Hewitt, I. J.; Madhu, N. T.; Chastanet, G.; Wernsdorfer, W.; Anson, C. E.; Benelli, C.; Sessoli, R.; Powell, A. K. *Angew. Chem.* **2006**, *118*, 1761. (g) Ishikawa, N. *Polyhedron* **2007**, *26*, 2147. (h) Lin, P.-H.; Burchell, T. J.; Clerac, R.; Murugesu, M. *Angew. Chem., Int. Ed.* **2008**, *47*, 8848. (i) AlDamen, M. A.; Clemente-Juan, J. M.; Coronado, E.; Mart-Gastaldo, C.; Gaita-Ario, A. *J. Am. Chem. Soc.* **2008**, *130*, 8874. (j) Hussain, B.; Savard, D.; Burchell, T. J.; Wernsdorfer, W.; Murugesu, M. *Chem. Commun.* **2009**, 1100. (k) Takamatsu, S.; Ishikawa, T.; Koshihara, S.; Ishikawa, N. *Inorg. Chem.* **2007**, *46*, 7250. (l) Gamer, M. T.; Lan, Y.; Roesky, P. W.; Powell, A. K.; Clrac, R. *Inorg. Chem.* **2008**, *47*, 6581. (m) Zheng, Y.-Z.; Lan, Y.; Anson, C. E.; Powell, A. K. *Inorg. Chem.* **2008**, *47*, 10813. (n) Westin, L. G.; Kritikos, M.; Caneschi, A. *Chem. Commun.* **2003**, 1012.

Published on Web 08/19/2009

Table 1. Crystal Data and Structure Refinements for **1**−**5**

	1	**2**	**3**
formula	$C_{54}H_{36}Br_2F_{36}Pr_2N_6O_{16}$	$C_{54}H_{38}Br_2F_{36}Sm_2N_6O_{16}$	$C_{54}H_{36}Br_2F_{36}Eu_2N_6O_{16}$
fw	2150.53	2171.42	2172.63
T (K)	113(2)	113(2)	113(2)
cryst syst	triclinic	triclinic	triclinic
space group	$P\bar{1}$	$P\bar{1}$	$P\bar{1}$
a (Å)	11.419(2)	11.440(2)	11.462(2)
b (Å)	11.527(2)	11.478(2)	11.482(2)
c (Å)	16.880(3)	16.827(3)	16.833(3)
α (deg)	94.83(3)	94.32(3)	94.74(3)
β (deg)	106.36(3)	106.94(3)	107.02(3)
γ (deg)	115.51(3)	115.85(3)	115.58(3)
V (Å^3)	1869.1(6)	1848.9(6)	1853.7(6)
Z	1	1	1
ρ [g/cm^3]	1.911	1.950	1.946
μ [mm^{-1}]	2.511	2.809	2.910
θ (deg)	2.02−27.56	2.05−25.02	2.03−25.02
index ranges	$-14 \le h \le 14$	$-13 \le h \le 12$	$-13 \le h \le 13$
	$-14 \le k \le 14$	$-13 \le k \le 13$	$-13 \le k \le 13$
	$-20 \le l \le 21$	$-16 \le l \le 20$	$-20 \le l \le 20$
reflns collected	15026	10684	16251
independent	8484	6469	6546
data/restraints	8484/338/663	6469/548/731	6546/324/770
GOF on F^2	1.003	1.030	1.005
R_1, ωR_2 [$I > 2\sigma(I)$]	0.0469, 0.1125	0.0486, 0.1286	0.0360, 0.0807
R_1, ωR_2 (all data)	0.0552, 0.1185	0.0563, 0.1330	0.0409, 0.0831

	4	**5**
formula	$C_{54}H_{36}Br_2F_{36}Tb_2N_6O_{16}$	$C_{27}H_{18}BrF_{18}TmN_3O_8$
fw	2186.55	1103.28
T (K)	293(2)	113(2)
cryst syst	triclinic	monoclinic
space group	$P\bar{1}$	$P2(1)/n$
a (Å)	11.611(2)	13.045(3)
b (Å)	11.654(2)	18.283(4)
c (Å)	16.915(3)	15.819(3)
α (deg)	107.84(3)	90
β (deg)	94.68(3)	94.53(3)
γ (deg]	115.28(3)	90
V (Å^3)	1909.2(6)	3761.1(13)
Z	1	4
ρ [g/cm^3]	1.902	1.948
μ [mm^{-1}]	3.035	3.559
θ (deg)	3.11−27.48	2.11−27.89
index ranges	$-15 \le h \le 15$	$-17 \le h \le 17$
	$-15 \le k \le 15$	$-18 \le k \le 24$
	$-20 \le l \le 21$	$-20 \le l \le 20$
reflns collected	19441	27096
independent	8730	8916
data/restraints	8730/477/719	8916/72/555
GOF on F^2	1.047	1.042
R_1, ωR_2 [$I > 2\sigma(I)$]	0.0648, 0.1695	0.0378, 0.0910
R_1, ωR_2 (all data)	0.0762, 0.1790	0.0439, 0.0948

rare-earth-radical-based complexes have been reported as single-chain magnets.[3e,f] Furthermore, since the first Dy(III)-radical-based molecule [Dy(hfac)$_3$NITpPy]$_2$ (hfac = hexafluoroacetylacetonate, NITpPy = 2-(4-pyridyl)-4,4,5,5-tetramethyl-4,5-dihydro-1H-imidazolyl-3-oxide) showing single-molecule magnetic (SMM) behavior was discovered in 2007,[3d] very little work has been done to date on this kind of system. SMMs based on 4f have been much less explored despite lanthanide ions having large intrinsic magnetic anisotropy,[4] especially rare-earth-radical-based systems.

The complex [Gd(hfac)$_3$(NIT-5-Br-3py)]$_2$ was previously reported by some of us.[5a] In this paper, we synthesized five other rare-earth-radical-based complexes, [Ln(hfac)$_3$(NIT-5-Br-3py)]$_2$ (Ln = Pr (**1**), Sm (**2**), Eu (**3**), Tb (**4**), Tm (**5**)), and described their crystal structures and magnetic properties. For complex **4**, the frequency dependence of the ac susceptibility suggests SMM behavior.

Experimental Section

Synthesis. The five compounds were synthesized following a procedure similar to that exemplified for **4** hereafter. A solution of Tb(hfac)$_3 \cdot 2H_2O$[3e] (82 mg, 0.1 mmol) in 15 mL of dry *n*-heptane was heated under reflux for 1 h. After that, the solution was cooled to about 65 °C, and a solution of NIT-5-Br-3py[5b] (31 mg, 0.1 mmol) in 5 mL of CH_2Cl_2 was added. The resulting mixture was stirred for 30 min and then cooled to room temperature. After filtration, the resulting solution was left at 4 °C for several days to give light violet elongated crystals suitable for X-ray

(5) (a) Xu, J.-X.; Ma, Y.; Xu, G.-F.; Wang, C.; Liao, D.-Z.; Jiang, Z.-H.; Yan, S.-P.; Li, L.-C. *Inorg. Chem. Commun.* **2008**, *11*, 1356. (b) Davis, M. S.; Morokuma, K.; Kreilick, R. W. *J. Am. Chem. Soc.* **1972**, *94*, 5588.

analysis. Crystal data and structure refinements for **1**−**5** are given in Table 1 (the selected bond lengths and angles have been placed in the Supporting Information). Anal. Calcd (**1**) for $C_{54}H_{36}Br_2F_{36}Pr_2N_6O_{16}$: C, 30.16; H, 1.69; N, 3.91. Found: C, 30.13; H, 1.58; N, 3.89%. Anal. Calcd (**2**) for $C_{54}H_{38}Br_2F_{36}Sm_2N_6O_{16}$: C, 29.87; H, 1.76; N, 3.87. Found: C, 29.66; H, 1.89; N, 3.91%. Anal. Calcd (**3**) for $C_{54}H_{36}Br_2F_{36}Eu_2N_6O_{16}$: C, 29.85; H, 1.67; N, 3.87. Found: C, 29.87; H, 1.91; N, 3.75%. Anal. Calcd (**4**) for $C_{54}H_{36}Br_2F_{36}Tb_2N_6O_{16}$: C, 29.66; H, 1.66; N, 3.84. Found: C, 29.60; H, 1.78; N, 3.89%. Anal. Calcd (**5**) for $C_{54}H_{36}Br_2F_{36}Tm_2N_6O_{16}$: C, 29.39; H, 1.64; N, 3.81. Found: C, 29.52; H, 1.58; N, 3.84%.

Crystal Structure Determination. Crystals of **1**−**5** were mounted on glass fibers. Determination of the unit cell and data collection were performed with Mo Kα radiation ($\lambda = 0.71073$ Å) on a Bruker SMART 1000 diffractometer and equipped with a CCD camera. The $\omega-\varphi$ scan technique was employed. The structures were solved primarily by direct method and second by Fourier difference techniques and refined by the full-matrix least-squares method. The computations were performed with the SHELXL-97 program.[6] Non-hydrogen atoms were refined anisotropically. The hydrogen atoms were set in calculated positions and refined as riding atoms with a common fixed isotropic thermal parameter. CCDC 716779, 701869, 701867, 716523, and 701868 contain the supplementary crystallographic data for complexes **1**−**5**, respectively. These data can be obtained free of charge via www.ccdc.cam.ac.uk/conts/retrieving.html (or from the Cambridge Crystallographic Data Center, 12 Union Road, Cambridge CB2 1EZ, U.K.; fax: (+44) 1223-336-033; e-mail: deposit@ccdc.cam.ac.uk).

Materials and Physical Techniques. All reagents and solvents employed were commercially available and used as received without further purification. Elemental analyses for C, H, and N were obtained at the Institute of Elemental Organic Chemistry, Nankai University. Variable-temperature magnetic susceptibilities were measured on a SQUID MPMS XL-7 magnetometer. Diamagnetic corrections were made with Pascal's constants for all of the constituent atoms.

Results and Discussion

Crystal Structures. The molecular structures of five complexes are similar, each of which is a cyclic dimer comprising two asymmetric units of [Ln(hfac)$_3$(NIT-5-Br-3py)] (Ln = Pr (**1**), Sm (**2**), Eu (**3**), Tb (**4**), Tm (**5**); the molecular structure of **4** is given in Figure 1). To each lanthanide(III) ion, there are eight coordination sites which are occupied by six oxygen atoms from the hfac ligand, one oxygen atom from the nitronyl nitroxide unit, and one nitrogen atom from the pyridine ring. The oxygen atoms from the radical and the nitrogen atom are coordinated to Ln(III) in a cis configuration. The nitronyl nitroxide moiety acts as a bridge ligand linking two Ln(III) ions by the oxygen atom of the N−O group and the nitrogen atom of the pyridine ring. The important bond lengths and angles for **1**−**5** are listed in Table 2.

Static Magnetic Properties. The effects of spin−orbit coupling and the crystal field in general play more important roles in the magnetism of lanthanide complexes. For such a Ln(III) ion, the $4f^n$ configuration is split into $^{2S+1}L_J$ spectroscopic levels by interelectronic repulsion and spin−orbit coupling. Each of these states is further split into Stark sublevels by the crystal field perturbation.

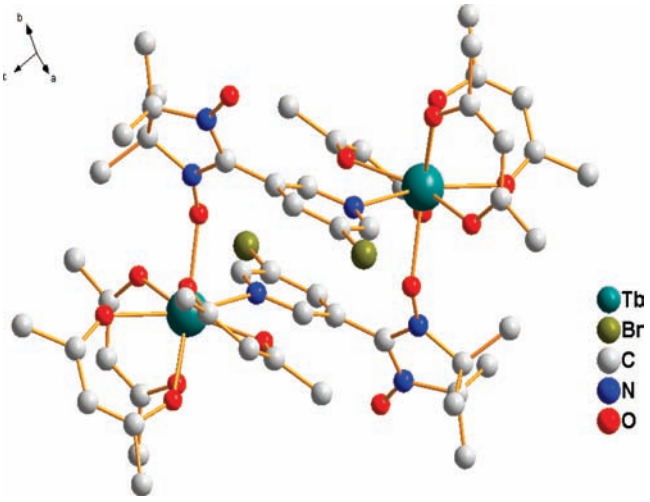

Figure 1. The molecular structure of **4**. Fluorine and hydrogen atoms are not shown for the sake of clarity.

For most of the Ln(III) ions, the energy separation between the $^{2S+1}L_J$ ground state and the first excited state is so large that only the ground state is thermally populated at room and low temperatures, except for the Sm(III) and Eu(III) ions, in which the excited states may be thermally populated because of the weak energy separation.[7]

Static Magnetic Properties for 1 and 5. The temperature dependence of magnetic susceptibilities for **1** and **5** are studied and shown in Figure S2 (Supporting Information). The μ_{eff} values of **1** and **5** at 300 K are 5.62 and 11.13 μ_B, in good agreement with that expected (5.61 and 10.97 μ_B) for two uncoupled Ln(III) ions ($^3H_4$, $g = 4/5$ for Pr(III) ion, and $^3H_6$, $g = 7/6$ for Tm(III) ion) and two organic radicals ($S = 1/2$). Upon cooling, the μ_{eff} values of **1** decrease and reach a minimum of 2.22 μ_B at 2 K, while the μ_{eff} values of **5** increase smoothly and reach a maximum at 16 K with a value of 11.49 μ_B and then sharply reach a minimum (8.13 μ_B) at 2 K.

A strictly theoretical treatment of magnetic properties for such a system cannot be carried out because of the large anisotropy of the Ln(III) ions. However, to obtain a rough quantitative estimate of the magnetic interaction parameters between paramagnetic species, the temperature-dependent magnetic susceptibilities were analyzed by an approximate model for **1** and **5** (in the Supporting Information), which suggested antiferromagnetic interactions between Pr^{III} and radicals in **1** and ferromagnetic interactions between Tm^{III} and radicals in **5**.

Static Magnetic Properties for 2 and 3. Figure 2a shows the plot of μ_{eff} versus T for a powder sample of **2** measured in the temperature range 2−300 K. The μ_{eff} value of **2** at 300 K is 3.29 μ_B. Upon cooling, μ_{eff} continuously decreases to reach a minimum of 0.88 μ_B at $T = 2$ K. The ^6H ground term for the Sm(III) ion is split by the spin−orbit coupling into six levels $E(J) = \lambda J(J+1)/2$ with the spin−orbit coupling parameter λ on the order of 200 cm^{-1} and $J = 5/2$, 7/2, 9/2, 11/2, 13/2, and 15/2. In addition to

(6) (a) Sheldrick, G. M. *SHELXS 97*; University of Göttingen: Göttingen, Germany, 1997. (b) Sheldrick, G. M. *SHELXL 97*; University of Göttingen: Göttingen, Germany, 1997.

(7) (a) Kahn, O. *Molecular Magnetism*; VCH: New York, 1993. (b) Li, Y.; Zheng, F.-K.; Liu, X.; Zou, W.-Q.; Guo, G.-C; Lu, C.-Z.; Huang, J.-S. *Inorg. Chem.* **2006**, *45*, 6308. (c) Kahn, M. L.; Sutter, J.-P.; Golhen, S.; Guionneau, P.; Ouahab, L.; Kahn, O.; Chasseau, D. *J. Am. Chem. Soc.* **2000**, *122*, 3413.

Table 2. The Important Bond Lengths and Angles for **1**−**5**

complexes	bond lengths (Ln−O_{Rad}) (Å)	bond lengths (Ln−N_{Py}) (Å)	range of bond lengths (Ln−O_{hfac}) (Å)	bond lengths (N_{Rad}−$O_{Rad(coordinated)}$) (Å)	bond lengths (N_{Rad}−$O_{Rad(uncoordinated)}$) (Å)	angle of O_{Rad}−Ln−N_{Py} (deg)	dihedral angle between the pyridine plane and the nitron-yl nitroxide N−C−N plane (deg)
Pr(1)	2.410(3)	2.703(4)	2.388(3)−2.473(3);	1.301(4)	1.265(5)	74.20(10)	52.6
Sm(2)	2.360(11)	2.67(2)	2.342(11)−2.433(11);	1.297(15)	1.265(17)	73.7(5)	54.1
Eu(3)	2.349(9)	2.66(2)	2.330(9)−2.417(9);	1.305(14)	1.267(15)	74.0(5)	53.9
Tb(4)	2.334(5)	2.642(5)	2.299(5)−2.391(5);	1.290(7)	1.252(8)	75.37(17)	51.7
Tm(5)	2.307(2)	2.573(3)	2.276(3)−2.329(2);	1.312(4)	1.265(4)	73.40(9)	50.1

the ground state $^6H_{5/2}$, the first ($^6H_{7/2}$) and even higher excited states can be considerably populated at room temperature.[7a,8] Therefore, the observed μ_{eff} value (3.29 μ_B) of **2** at room temperature is larger than the expected value (2.73 μ_B) for two uncoupled Sm(III) ions ($^6H_{5/2}$, $g = 2/7$) and two organic radicals ($S = 1/2$). On lowering the temperature, μ_{eff} values decrease due to the thermal depopulation of the excited levels. Assuming that the crystal field spitting is small in this case, the magnetic susceptibility of χ_{Sm} may be expressed as in eq 1.

$$\chi_{Sm} = \frac{N\beta^2}{3kTx}\frac{BB}{CC} \tag{1}$$

$$BB = (2.143x+7.347) + (42.92x+1.641)e^{(-7/2x)} + (283.7x-0.6571)e^{(-8x)} + (620.6x-1.94)e^{(-27/2x)} + (1122x-2.835)e^{(-20x)} + (1813x-3.556)e^{(-55/2x)}$$

$$CC = 3 + 4e^{(-7/2x)} + 5e^{(-8x)} + 6e^{(-27/2x)} + 7e^{(-20x)} + 8e^{(-55/2x)}$$

$$x = \frac{\lambda}{kT}$$

$$\chi_{Rad} = \frac{Ng_R^2\beta^2}{3kT}\frac{1}{2}\left(\frac{1}{2}+1\right) \quad (g_R = 2) \tag{2}$$

$$\chi_{MF} = \frac{\chi_{total}}{1-(2zJ'/Ng^2\beta^2)\chi_{total}} \tag{3}$$

The magnetic susceptibility of **2** is treated as a sum of the contributions of two Sm(III) ions and two radicals ($\chi_{total} = 2\chi_{Rad} + 2\chi_{Sm}$). Then, taking into account the interaction between paramagnetic species, a correction for a molecular field can be made (eq 3). The least-squares fit to the data (35−300 K) leads to $\lambda = 299\ cm^{-1}$,[1,10] $zJ' = -7.7\ cm^{-1}$, $g = 1.38$, and $R = \sum(\chi_{obsd} - \chi'_{cacld})^2/\sum(\chi_{obsd})^2 = 2.1 \times 10^{-3}$ for **2**. (Data below 35 K were omitted in the fitting because small crystal field splittings are likely to influence the data in this temperature range.) The negative zJ' suggests antiferromagnetic interactions between the paramagnetic ions (Sm(III) ions and radicals) in the complex.

The experimental thermal dependence of μ_{eff} for **3** in the range of 2−300 K is shown in Figure 2b. The μ_{eff} value of 5.58 μ_B at room temperature continuously decreases with the temperature to a value of 1.75 μ_B at 2 K. The ground state $^7F_0$ of Eu(III) ($4f^6$, $J = 0$, $S = 3$, $L = 3$, $^7F_0$) is nonmagnetic, but the observed μ_{eff} value (5.58 μ_B) of **3** at room temperature is larger than the expected value (2.45 μ_B) for two organic radicals. This is due to a certain amount of magnetic moment from the excited state ($^7F_1$, $^7F_2$, $^7F_3$, $^7F_4$, $^7F_5$, $^7F_6$). The decrease in μ_{eff} values on lowering the temperature attributes to the thermal depopulation of these excited levels. Because only the nonmagnetic ground state $^7F_0$ of Eu(III) is populated, there is no Stark sublevel from the ligand field. Thus, χ_{Eu} can be analyzed with the expression given in eq 4.

$$\chi_{Eu} = \frac{N\beta^2}{3kTx}\frac{BB}{CC} \tag{4}$$

$$BB = 24 + \left(\frac{27}{2}x - \frac{3}{2}\right)e^{(-x)} + \left(\frac{135}{2}x - \frac{5}{2}\right)e^{(-3x)} + \left(189x - \frac{7}{2}\right)e^{(-6x)} + \left(405x - \frac{9}{2}\right)e^{(-10x)} + \left(\frac{1485}{2}x - \frac{11}{2}\right)e^{(-15x)} + \left(\frac{2457}{2}x - \frac{13}{2}\right)e^{(-21x)}$$

$$CC = 1 + 3e^{(-x)} + 5e^{(-3x)} + 7e^{(-6x)} + 9e^{(-10x)} + 11e^{(-15x)} + 13e^{(-21x)}$$

$$x = \frac{\lambda}{kT}$$

$$\chi_{Rad} = \frac{Ng_R^2\beta^2}{3kT}\frac{1}{2}\left(\frac{1}{2}+1\right) \quad (g_R = 2) \tag{5}$$

$$\chi_{total} = 2\chi_{Rad} + 2\chi_{ln} \tag{6}$$

$$\chi_{MF} = \frac{\chi_{total}}{1-(2zJ'/Ng^2\beta^2)\chi_{total}} \tag{7}$$

where λ is the spin−orbit coupling parameter; the zJ' parameter based on the molecular field approximation is introduced (eq 7) to roughly simulate the magnetic interactions between the paramagnetic species.[9] The magnetic susceptibility of **3** is treated as a sum (eq 6) of the contributions of two Eu(III) ions (eq 4) and two radicals (eq 5). Then, taking into account the interaction between paramagnetic species, a correction for a molecular field can be made (eq 7). The least-squares fit to the data leads to $\lambda = 332\ cm^{-1}$,[1,10] $zJ' = -1.2\ cm^{-1}$, $g = 1.91$, and $R = \sum(\chi_{obsd} - \chi'_{cacld})^2/\sum(\chi_{obsd})^2 = 2.0 \times 10^{-3}$ for **3**. The value of zJ' reveals weak antiferromagnetic

(8) Przychodzén, P.; Lewínski, K.; Pełka, R.; Bałanda, M.; Tomala, K.; Sieklucka, B. *Dalton Trans.* **2006**, 625.

(9) (a) Liao, Y.; Shum, W. W.; Miller, J. S. *J. Am. Chem. Soc.* **2002**, *124*, 9336. (b) O'Connor, C. J. *Prog. Inorg. Chem.* **1982**, *29*, 203.

(10) Hinatsu, Y.; Doi, Y. *Bull. Chem. Soc. Jpn.* **2003**, *76*, 1093.

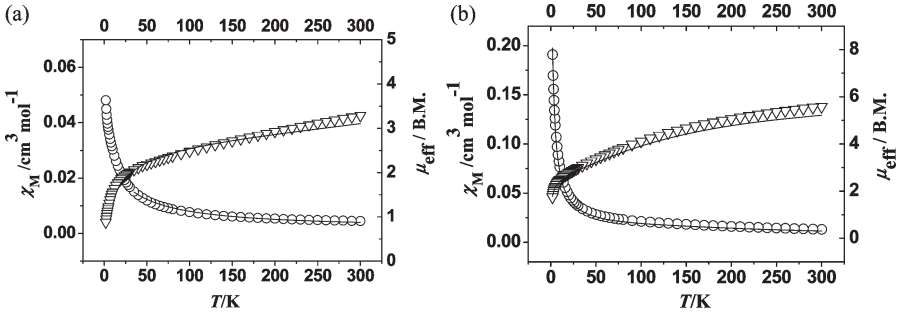

Figure 2. χ_M (○) versus T and $\chi_M T$ (▽) versus T plots for **2** (a) and **3** (b). The solid lines represent the theoretical.

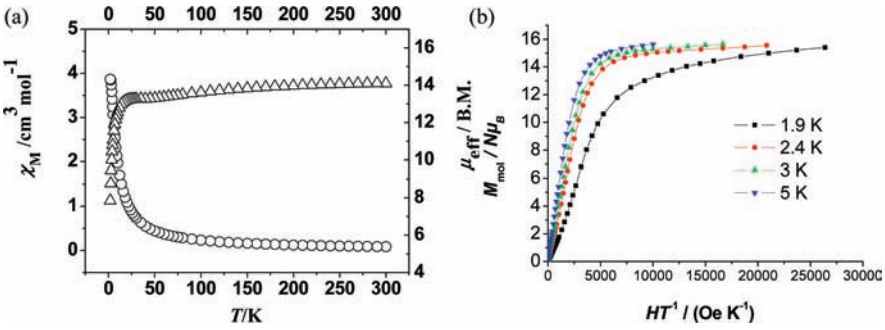

Figure 3. (a) χ_M (○) versus T and μ_{eff} (Δ) versus T plots for **4**. (b). $M_{mol}/N\mu_B$ versus HT^{-1} plot at low temperatures for **4**.

interaction between the paramagnetic ions (Eu(III) ions and radicals).

Static Magnetic Properties for 4. The static magnetic moment of polycrystalline powder of the compound was measured using a SQUID magnetometer in the temperature range 2−300 K at 1000 Oe (Figure 3). The μ_{eff} versus T measurements performed on the Tb(III) compound show a room temperature value of 14.10 μ_B, slightly higher than that expected (13.96 μ_B) for two uncoupled Tb(III) ($^7F_6$, $g_J = 3/2$) and two organic radicals ($S = 1/2$). On decreasing the temperature, the μ_{eff} values decrease steadily above 14 K and then decrease sharply to 7.86 μ_B at 2.0 K. This magnetic behavior may be ascribed to the exchange interaction between the paramagnetic ions (Rad−Rad, Rad−Tb(III), Tb(III)−Tb(III)) combined with the crystal field and spin−orbit effect, which is important for Tb(III) behaving intrinsically anisotropic. At present, it is not possible to quantify the different contributions (in the Supporting Information),[11] but the crystal field and spin−orbit effect may be dominant due to the completed 5s and 5p subshells shielding 4f electrons and be crucial for the SMM behavior for the present complex (see below).

The $M_{mol}/N\mu_B$ versus H below 5 K shows a rapid increase in the magnetization at low magnetic fields (Figure S1 in the Supporting Information). At higher fields, $M_{mol}/N\mu_B$ increases up to 15.37 μ_B at 1.9 K and 50 000 Oe but does not reach the expected saturation of 16 $N\beta$ (9 $N\beta$ for each Tb(III) ion and 1 $N\beta$ for each radical; the ground state is given by Tb↑—Rad↓—Tb↑—Rad↓) due to the crystal effect on the Tb(III) ion. This high-field variation and the nonsuperposition on a single mastercurve of the $M_{mol}/N\mu_B$ versus HT^{-1} data (Figure 3b) imply the presence of low-lying excited sta-5tes and a significant magnetic anisotropy.[4h] Nevertheless, it is worth noting that the M_{mol} versus H data do not exhibit a hysteresis effect above 1.8 K, which may be caused by the presence of a relatively fast zero-field relaxation.[4h]

Dynamic Magnetic Properties for 4. The dynamic magnetic susceptibility measurements of the complexes were performed in the range of 100−1490 Hz, and only complex **4** displays clear frequency dependence and peaks in χ' versus T and χ'' versus T plots in zero static field (Figure 4). The frequency dependence of the in-phase and out-of-phase components of ac magnetic susceptibility χ_M', χ_M'' at $T < 4$K under zero dc field, indicates the onset of slow relaxation, which is a diagnosis of a SMM. Analysis of the frequency dependence of the χ_M'' peaks through Arrhenius law ($\tau = \tau_0 \exp(-U_{eff}/k_BT)$) permits estimation of magnetization−relaxation parameters, and best fitting (Figure 5) affords the parameter values: the preexponential factor $\tau_0 = 5.9 \times 10^{-9}$ s and the energy barriers for the relaxation of the magnetization $U_{eff}/k_B =$ 28.7 K ($R = 0.999$). The existence of a single relaxation process is supported by the representation of the χ_M'' versus χ_M' at 1.9 and 2.5 K in the Cole−Cole plot (Figure 6).

The semicircle Cole−Cole diagram can be fitted by a generalized Debye model:[12]

$$\chi_{(\omega)} = \chi_s + \frac{\chi_T - \chi_s}{1+(i\omega\tau)^{1-\alpha}}$$

(11) Aronica, C.; Pilet, G.; Chastanet, G.; Wernsdorfer, W.; Jacquot, J. F.; Luneau, D. *Angew. Chem., Int. Ed.* **2006**, *45*, 4659.

(12) (a) Cole, K. S.; Cole, R. H. *J. Chem. Phys.* **1941**, *9*, 341. (b) Dekker, C; Arts, A. F. M.; de Wijn, H. W.; van Duyneveldt, A. J.; Mydosh, J. A. *Phys. Rev. B* **1989**, *40*, 11243. (c) Aubin, S. M. J.; Sun, Z.; Pardi, L.; Krzystek, J.; Folting, K.; Brunel, L. C.; Rheingold, A. L.; Christou, G.; Hendrickson, D. N. *Inorg. Chem.* **1999**, *38*, 5329. (d) Ishii, N.; Okamura, Y.; Chiba, S.; Nogami, T.; Ishida, T. *J. Am. Chem. Soc.* **2008**, *130*, 24.

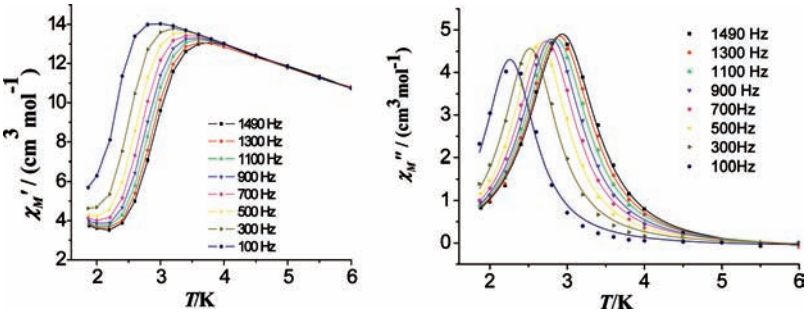

Figure 4. Temperature dependence of the in-phase (left) and out-of-phase (right) components of the ac magnetic susceptibility for complex **4** under zero dc field. Solid lines are eye guides.

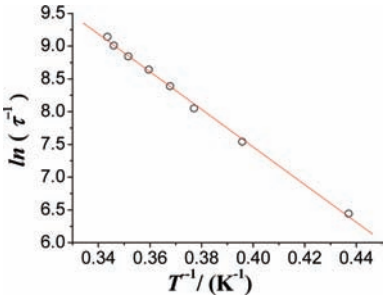

Figure 5. Plot of ln(τ^{-1}) versus (T^{-1}) for complex **4**. The solid line is a least-squares fitting to the Arrhenius equation.

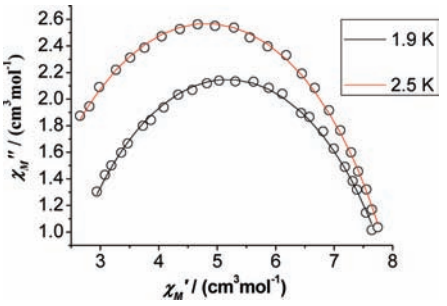

Figure 6. Cole−Cole diagram at 1.9 and 2.5 K for complex **4**. The solid lines represent fitting with an extended Debye model (see text).

where χ_T is the isothermal susceptibility, χ_S is the adiabatic susceptibility, ω is the frequency of the ac field, and τ is the relaxation time of the system, giving $\alpha = 0.23$ ($R^2 = 0.996$, $T = 1.9$ K) and 0.19 ($R^2 = 0.998$, $T = 2.5$ K). The small values are compatible with SMM behavior.[13] Furthermore, the frequency dependence of the peak temperature in χ_M', $\varphi = (\Delta T_p/T_p)/\Delta(\log \omega)$ (where ΔT_p is the difference between the higher and lower blocking temperatures corresponding to two different frequency values (100 and 1300)), was 0.21, which excludes the possibility of a spin glass ($0.01 < \varphi < 0.08$).[12d,13,14]

Compared with the first Dy(III)-radical-based molecule $[Dy(hfac)_3NITpPy]_2$, the Tb(III) complex has an analogous structure containing two asymmetric units, in which the nitronyl nitroxide radical acts as a bidentate ligand toward Tb(III) through the nitrogen atom of the pyridine ring and the oxygen atom of the N−O group. The Tb(III) complex displays clear frequency dependence and peaks in χ' versus T and χ'' versus T plots in zero static field. However, the Dy(III) complex displays peaks in χ'' only in a external static magnetic field ($H = 2000$ Oe), which must be applied to suppress the quantum tunneling process. In addition, the Tb(III) complex has a significantly higher barrier ($U_{eff}/k_B = 28.7$ K) than that of the Dy(III) complex ($U_{eff}/k_B = 13.7$ K).

The origin of the mechanism of SMM behavior in lanthanide-containing complexes is different from that of the 3d metal clusters.[4e,k,15] The SMM behavior for the $[Tb(hfac)_3(NIT\text{-}5\text{-}Br\text{-}3py)]_2$ may be mainly ascribed to its less symmetrical ligand field splitting pattern:[4e,k,15] the ligand field made by the radicals and hfac can lift the 13-fold degeneracy of the $J = 6$ ground multiplet of the Tb(III) ion and yield a situation where the lowest substates formally corresponding to $Jz = \pm 6$ are considerably separated (by ca. 400 cm^{-1}) from the rest of the substates. This can lead to a strong uniaxial magnetic anisotropy and higher thermal barrier between $Jz = +6$ and $Jz = -6$. However, the magnetic interactions of Tb(III) ions and the radicals could enhance the resulting uniaxial anisotropy.[11]

Conclusion

In conclusion, we report five new complexes based on rare-earth radicals. The results show that these complexes have similar structures. Each of them is a cyclic dimer comprising two asymmetric units of $[Ln(hfac)_3(NIT\text{-}5\text{-}Br\text{-}3py)]$. The nitronyl nitroxide moiety acts as a bridge linking two Ln(III) ions by the oxygen atom of the N−O group and the nitrogen atom of the pyridine ring. The temperature dependencies of magnetic susceptibilities for five complexes are studied. Furthermore, the frequency dependence of the ac susceptibility justifies that complex **4** exhibits SMM behavior.

(13) Gatteschi, D.; Sessoli, R.; Villain, J. *Molecular Nanomagnets*; Oxford University Press: New York, 2006; pp 69−75.

(14) Hibbs, W.; Rittenberg, D. K.; Sugiura, K.-i.; Burkhart, B. M.; Morin, B. G.; Arif, A. M.; Liable-Sands, L.; Rheingold, A. L.; Sundaralingam, M.; Epstein, A. J.; Miller, J. S. *Inorg. Chem.* **2001**, *40*, 1915.

(15) (a) Takamatsu, S.; Ishikawa, N. *Polyhedron* **2007**, *26*, 1859. (b) Sugita, M.; Ishikawa, N.; Ishikawa, T.; Koshihara, S.; Kaizu, Y. *Inorg. Chem.* **2006**, *45*, 1299. (c) Ferbinteanu, M.; Kajiwara, T.; Choi, K.-Y.; Nojiri, H.; Nakamoto, A.; Kojima, N.; Cimpoesu, F.; Fujimura, Y.; Takaishi, S.; Yamashita, M. *J. Am. Chem. Soc.* **2006**, *128*, 9008. (d) Ishikawa, N.; Sugita, M.; Wernsdorfer, W. *J. Am. Chem. Soc.* **2005**, *127*, 3650. (e) Ishikawa, N.; Iino, T.; Kaizu, Y. *J. Am. Chem. Soc.* **2002**, *124*, 11440. (f) Ishikawa, N.; Sugita, M.; Wernsdorfer, W. *Angew. Chem., Int. Ed.* **2005**, *44*, 2931. (g) Ueki, S.; Ishida, T.; Nogami, T.; Choi, K.-Y.; Nojiri, H. *Chem. Phys. Lett.* **2007**, *440*, 263. (h) Yamaguchi, T.; Sunatsuki, Y.; Ishida, H.; Kojima, M.; Akashi, H.; Re, N.; Matsumoto, N.; Pochaba, A.; Mrozi ski, J. *Inorg. Chem.* **2008**, *47*, 5736.

Acknowledgment. This work was supported by the National Natural Science Foundation of China (Nos. 20631030, 20871113), National Basic Research Program of China (973 Program, 2007CB815305), and Tianjin National Natural Science Foundation (No. 09JCYBJC05500).

Supporting Information Available: X-ray crystallographic files (CIF), selected bond lengths and angles for **1**−**5**, $M_{mol}/N\mu_B$ versus H plot at low temperatures, and temperature-dependent magnetic susceptibilities fitted by an approximate model for **1** and **5**. This material is available free of charge via the Internet at http://pubs.acs.org.